

# Using Unmanned Vehicles With Instrumented Bug Zappers To Detect & Eliminate Mosquitoes

Mary Burbage, An Nguyen, Kyle Walker, Nhan Phung, Vinh Truong, Erik Van Aller and Aaron Becker

**Abstract**—Mosquitoes are a vector for several deadly diseases which are responsible for killing millions of people each year. Popular methods to control mosquitoes such as insecticides are effective, but they introduce long-term damage to the environment. Traditional electrified screens (bug zappers) use UV light to attract pests but have a large bycatch of non-pest insects. This paper introduces techniques using electrified screens (bug zappers) mounted on unmanned vehicles to autonomously seek out and eliminate mosquitoes in their breeding grounds. Instrumentation on the bug zappers logs the GPS location, altitude, weather details, and time of each mosquito elimination. Mosquito control offices could use this information to analyze the insects' activities. The device can be mounted on a remote controlled or autonomous unmanned vehicle. If autonomous, the vehicle can use the data collected from the electrified net as feedback to improve the effectiveness of the motion plan. This paper examines design considerations, presents a working prototype system of drone and instrumented bug zapper, and introduces a simulator for swarms of mosquitoes and a mosquito-eliminating drone.

## I. INTRODUCTION

Mosquito-borne diseases kill millions of humans each year. Popular methods to control mosquitoes such as insecticides are effective, but they introduce long-term damage to the environment. Traditional electrified screens (bug zappers) use UV light to attract pests but have a large bycatch of non-pest insects. This paper introduces techniques using bug zappers mounted on unmanned vehicles to autonomously seek out and eliminate mosquitoes in their breeding grounds and swarms. Instrumentation on the bug zappers logs the GPS location, altitude, weather details, and time of each mosquito hit. Mosquito control offices can use this information to analyze the insects' activities. The device can be mounted on a remote-controlled or autonomous unmanned vehicle. If autonomous, the vehicle can use the data collected from the electrified net as feedback to improve the effectiveness of the motion plan.

Initial work simulates a large number of mosquitoes within a rectangular area. Each mosquito obeys a biased random walk flight pattern. Each mobile robot is capable of eliminating any modeled mosquito that intersects its path. The mobile robots can detect the time each mosquito is eliminated, share this information with neighboring drones, and use this data as feedback for a motion policy.

M. Burbage, A. Nguyen, K. Walker, N. Phung, V. Truong, E. Van Aller, and A. Becker are with the ECE Department at the University of Houston, TX. [atbecker@uh.edu](mailto:atbecker@uh.edu)

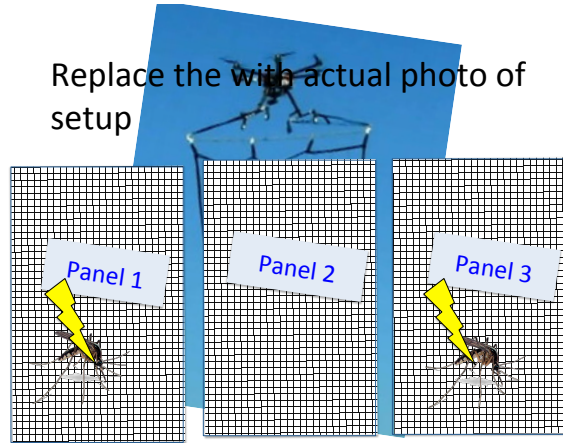


Fig. 1. A multi-copter drone carrying a high-voltage, instrumented bug-zapping screen. An onboard microcontroller monitors the voltage across the screen and records the time, GPS location, altitude, and weather information for each mosquito strike.

substitute real drone picture

## II. RELATED WORK

### A. Mosquito Control Solutions

Mosquito control has a long history of efforts associated both with monitoring mosquito populations [1] and with eliminating mosquitoes. The work involves both draining potential breeding grounds and destroying living mosquitoes [2]. An array of insecticidal compounds has been used with different application methods, concentrations, and quantities, including both larvicides and compounds directed at adult mosquitoes [3].

Various traps have been designed to capture and/or kill mosquitoes with increasing sophistication in imitating human bait as designers strive to achieve a trap that can rival the attraction of a live human [4]. In recent history, methods have also included genetically modifying mosquitoes so that they either cannot reproduce effectively or cannot transmit diseases successfully [5], and with the recent genomic mapping of mosquito species, new ideas for more targeted work have been formulated [6].

### B. Robotic Pest Management

As GPS technology has flourished and data processing has become cheaper and more readily available, researchers have explored options for implementing the new technologies in

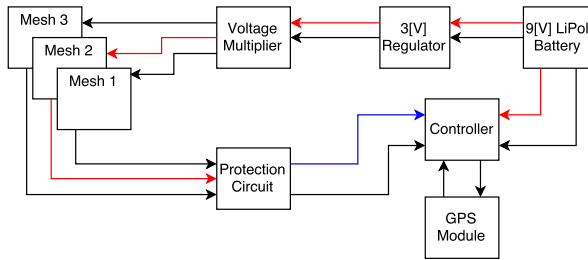


Fig. 2. Block diagram of microcontroller and bug zapper.

breeding ground removal [7] and more effective insecticide dispersion [8]. Even optical solutions have been considered, including laser containment [9] or, by extension, exclusion and laser tracking and extermination [10].

### C. Robotic coverage

Robotic coverage has a long history. The basic problem is one of designing a path for a robot that ensures the robot visits within  $r$  distance of every point on the workspace. For an overview see [11]. This work has been extended to use multiple coverage robots in a variety of ways, including using simple behaviors for the robots [12], [13]. The key difference in the mosquito coverage problem is that the mosquitoes can move, recontaminating an area previously cleared. We instead have a probability of coverage, as in [14]. This is closely related to the art gallery problem [15] but with limited range of visibility.

## III. DESIGN

### A. Electronics

Fig. 2 shows a block diagram of the control circuit. The system is powered by a 9 V Lithium Polymer battery applied directly to the controller. The 9 V supply is also regulated down to 3 V and applied to the voltage multiplier circuit that powers the mesh of the net, as shown in Fig. 3. The net output is a high voltage that a protection circuit steps down to a suitable level for the ADC of the controller. The controller utilizes a GPS shield for monitoring the location and altitude as well as a real time clock to timestamp each data point collected from the system.

A circuit diagram of both the bug zapper and the probe is shown in Fig. 3. The bug zapper (shown on the left) uses a BJT (Q1) and center tap transformer to invert a DC input voltage to AC and apply it to the primary winding of a step-up transformer (1:1000). The voltage at the secondary winding of the transformer is boosted and rectified to a high voltage output capacitor that is applied to the inner layer of the mesh. The probe (shown on the right) uses a voltage divider to lower the voltage so that it can be monitored by the microcontroller. A Zener diode (D4) placed in parallel protects the ADC input.

The screen is constructed with two layers of wire mesh with 3.6 mm openings with a layer of wire mesh with 0.74 mm openings suspended between them. A balsa wood frame insulates the outer meshes from the inner mesh. This mesh

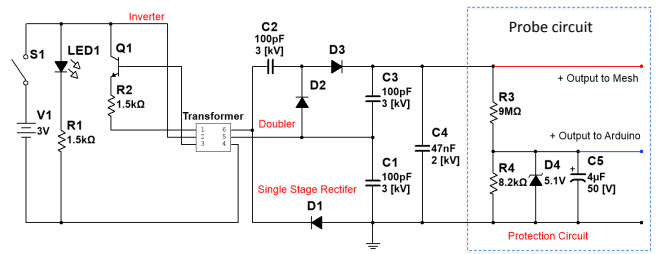


Fig. 3. Circuit diagram of the bug zapper and probe circuit.

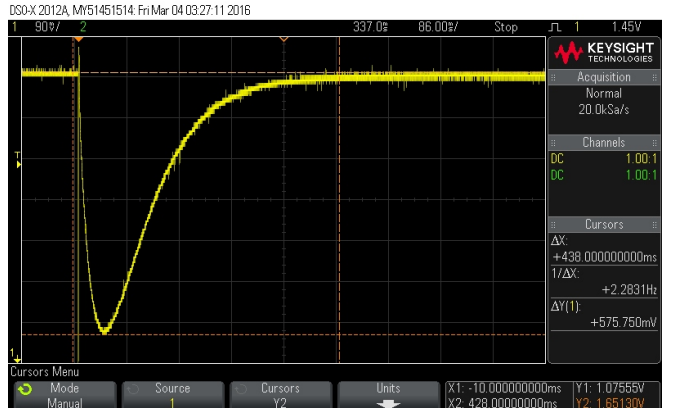


Fig. 4. Voltage trace as a pair of insects contact the bug-zapping screen. They cause a voltage deflection of 575 mV that recovers within 400 ms.

arrangement weighs  $1633 \text{ g/m}^2$ . The payload that the multi-copter can reliably carry is compared to the preferred width to find a size that satisfies the requirements.

### B. Energy Budget

how many mAh to keep an LxL screen charged? How many mAh to kill one mosquito: describe the experiment procedure and extrapolate the results

### C. Location of screen

The drone must carry the bug-zapping screen, and the location of this screen determines the efficacy of the mosquito drone, measured in mosquitoes eliminated per second of flight time.

To hover, the drone must push sufficient air down with velocity  $v_d$  to apply a force that cancels the pull of gravity. The drone has mass  $m_d$  and has a square-shaped cross section of size  $d_d \times d_d$ . The mass flow of air through the drone's props is equal to the product of the change in velocity of the air, the density of the air  $\rho_a$ , and the cross sectional area.

We assume that air above the multi-copter is quiescent, so the change in velocity of the air is  $v_d$  m/s.

$$\text{Force gravity} = (\text{mass flow}) \cdot \text{air velocity}$$

$$m_d \cdot g = (v_d \cdot \rho_a \cdot d_d^2) \cdot v_d \quad (1)$$

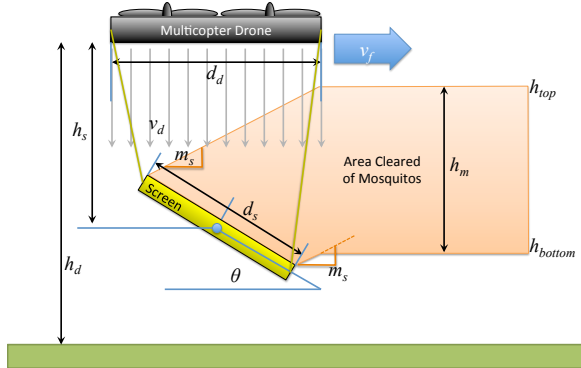


Fig. 5. The drone suspends a square bug-zapping screen beneath it. Propwash pushes incoming mosquitoes downwards, and the drone clears a volume  $h_m \times d_s \times v_f$ .

Then the propwash, the velocity of air beneath the drone, is

$$v_d = \sqrt{\frac{m_d g}{\rho_a d_d^2}} \quad (2)$$

The drone testing site in Houston, Texas is 15 m above sea level. At sea level the density of air  $\rho_a$  is 1.225 kg/m<sup>3</sup>. The 3DR Solo drone weighs 2 kg with diameter 0.71 m [16]. The acceleration due to gravity is 9.871  $\frac{m}{s^2}$ . Substituting these values into (2) gives  $v_d = 5.6$  m/s.

For manufacturing ease, the electrified screen is a square measuring  $d_s$  on each side. The mosquito species we are initially targeting fly at low altitude, so the screen is suspended a distance  $h_s$  beneath the drone flying at height  $h_d$ . Suspending this screen beneath the drone improves efficiency because a hanging screen requires less weight than a rigid frame to hold the screen above the drone. This screen can be suspended at any desired angle  $\theta$  in comparison to horizontal, as shown in Fig. 5. A key question is what distance  $h_s$  the screen should be suspended from the drone, and the optimal angle  $\theta$ . The goal is to clear the greatest volume of mosquitoes per second, a volume defined by the drone forward velocity  $v_f$  and the cross sectional area  $h_m \times d_s$  cleared by the screen, as shown in Fig. 6.

Due to propwash, a mosquito in level flight will fall relative to the drone at a rate of  $v_d/v_f$ . As shown in Fig. 5, we can extend lines with slope  $v_d/v_f$  from the screen's trailing edge to  $h_{top}$  and from the leading edge to  $h_{bottom}$

$$\begin{aligned} h_{top} &= h_d - h_s + \frac{d_s}{2} \sin(\theta) + \frac{d_d + d_s \cos(\theta)}{2} \frac{v_d}{v_f} \\ h_{bottom} &= h_d - h_s - \frac{d_s}{2} \sin(\theta) + \frac{d_d - d_s \cos(\theta)}{2} \frac{v_d}{v_f} \\ h_m &= h_{top} - h_{bottom} = d_s \left( \frac{v_d}{v_f} \cos(\theta) + \sin(\theta) \right) \end{aligned} \quad (3)$$

The optimal angle is therefore a function of forward and

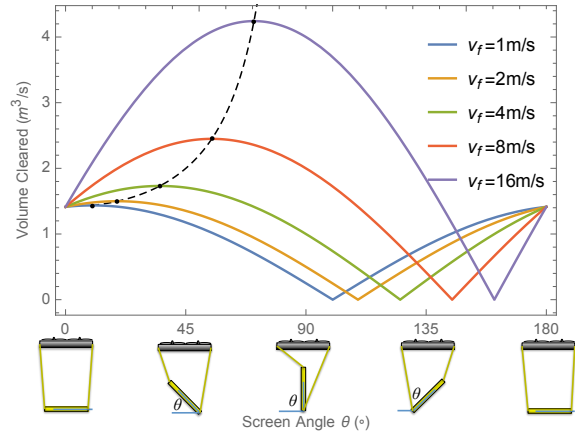


Fig. 6. The volume cleared by a drone is a function of screen angle  $\theta$  and forward velocity  $v_f$ . The dotted line shows the optimal angle given in (4).

propwash velocity:

$$\theta = \text{ArcTan} \left( \frac{v_f}{v_d} \right) \quad (4)$$

To ensure the maximum number of mosquitoes are collected, the screen must be sufficiently far below the drone  $h_s > \frac{d_s}{2} \sin(\theta) + \frac{d_d + d_s \cos(\theta)}{2} \frac{v_d}{v_f}$  and the bottom of the screen must not touch the ground,  $h_d > h_s + \frac{d_s}{2} \sin(\theta)$ .

Changing the flying height  $h_d$  of the drone will target different mosquito populations because mosquitoes are not distributed uniformly vertically. Gillies and Wilkes demonstrated this with a series of experiments counting mosquitoes caught in suction traps at various levels above ground in open grassland in the Gambia. These experiments showed that different species of mosquitoes prefer to fly at different heights [17].

#### IV. SIMULATION

Before launching a fully-instrumented drone, this concept was simulated using MATLAB code. One thousand mosquitoes are randomly placed within a square area one hundred meters on a side. Each mosquito moves according to a biased random walk at a speed up to 0.4 m/s and with a direction heading biased toward the greenest of the pixels surrounding its current position. This imitates the live mosquitoes' preference for vegetative areas. In order to allow the mosquito positions to be more natural, the mosquito movement routine runs five thousand times, simulating 1.4 hours of flying time, before the robot begins to search. Because mosquitoes do not care about boundaries, the toroidal assumption keeps them in the workspace.

Two different routines handle the robot's path. The first uses a random bounce algorithm. The robot begins in the center of the workspace and moves with a heading that varies randomly up to  $\pm 0.2$  rad off of its previous heading and bounces off the perimeter of the workspace with a random heading equally biased around all points of the circle except those outside the workspace. The velocity is set at a prescribed speed.

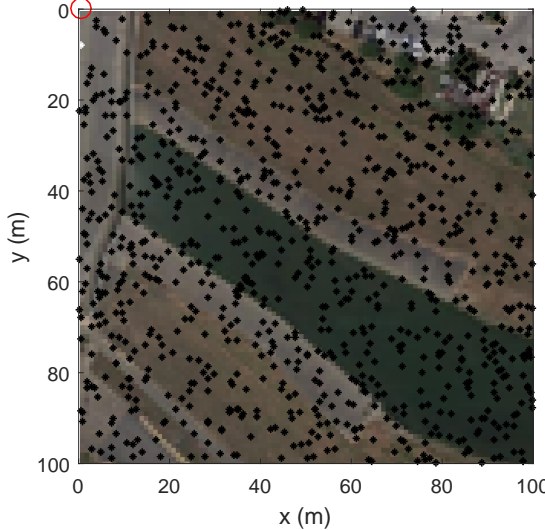


Fig. 7. A 100x100m image with one thousand simulated mosquitoes (black markers). The mosquitoes have had 1.5 hours to bias themselves toward green areas of the image. The robot (red circle) is shown at the upper left corner, preparing to start a bug-zapping run.

The second algorithm uses a boustrophedon path. The robot begins in one corner of the workspace and methodically progresses back and forth, advancing one screen width at each turn. If it covers the entire field in the allotted time, it begins covering the field again.

In order to keep the routines comparable, the robots use the same speed and same number of iterations. These simulations used 12 m/s and fifteen minutes of flying time. They also used the same image for biasing the mosquito flight.

For the main body of the simulation, a loop runs a series of iterations in which each mosquito moves one step and the robot moves one step. In that step, the path traced by the bug-zapping screen is calculated, and any mosquitoes in that path are considered to have been killed.

One hundred trials were performed with each coverage path and the results evaluated. The boustrophedon successfully covered the entire field in every trial ( $\mu=100\%$ ,  $\sigma=0\%$ ) and exhaustively covered a portion of the area a second time, while the random bounce covered only 67.9% of the field ( $\mu=67.9\%$ ,  $\sigma=1.0\%$ ) with an unknown amount of overlap. As a result, the boustrophedon killed significantly more mosquitoes ( $\mu=87.7\%$ ,  $\sigma=1.1\%$ ) than the random bounce ( $\mu=68.6\%$ ,  $\sigma=2.7\%$ ). In fact, the smallest number of mosquitoes killed in 100 trials by the boustrophedon (84.1%) was considerably larger than the largest number killed by the random bounce (75.1%).

## V. EXPERIMENT

Before mounting an instrumented screen to a drone, a proof of concept experiment used three commercial bug zappers mounted on a pole with two controllers and a GPS tracker. The circuits were powered with a 9 V battery as described above. One controller logged the GPS data at one

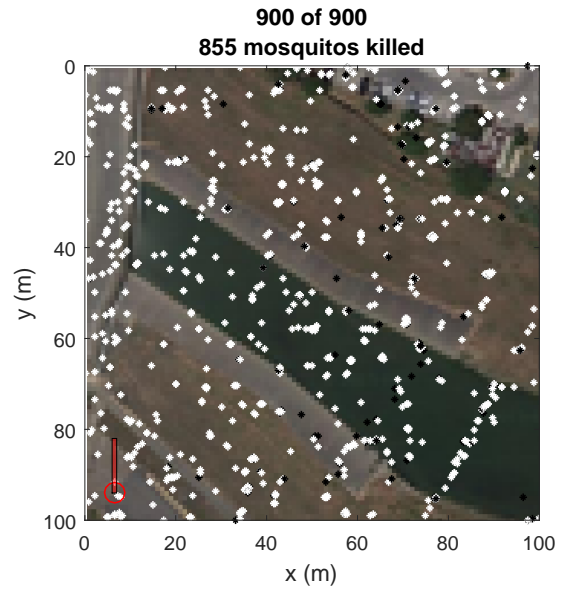


Fig. 8. A 100x100m image with the robot (red circle) and the area swept out by the bug-zapping net in a time step (red rectangle) shown along with a population of a thousand mosquitoes. Those that were killed during the simulation are shown in white, and those that survived it are shown in black.

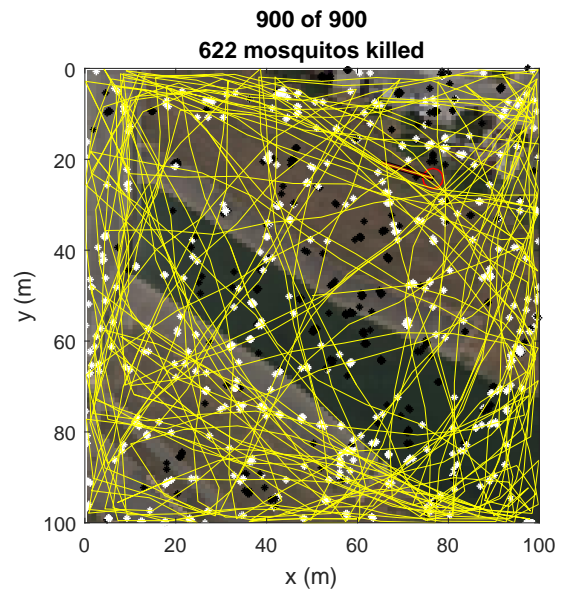


Fig. 9. Random bounce robot path (yellow lines) overlaid upon a 100x100m image. The robot (red circle) and the area swept out by the bug-zapping net in a time step (red rectangle) are shown along with a population of a thousand mosquitoes. Those that were killed during the simulation are shown in white, and those that survived it are shown in black.

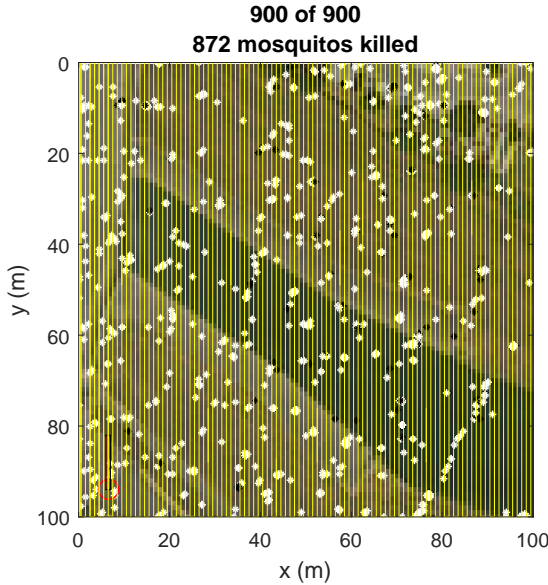


Fig. 10. Boustrophedon robot path (yellow lines) overlaid upon a 100x100m image. The robot (red circle) and the area swept out by the bug-zapping net in a time step (red rectangle) are shown along with a population of a thousand mosquitoes. Those that were killed during the simulation are shown in white, and those that survived it are shown in black.

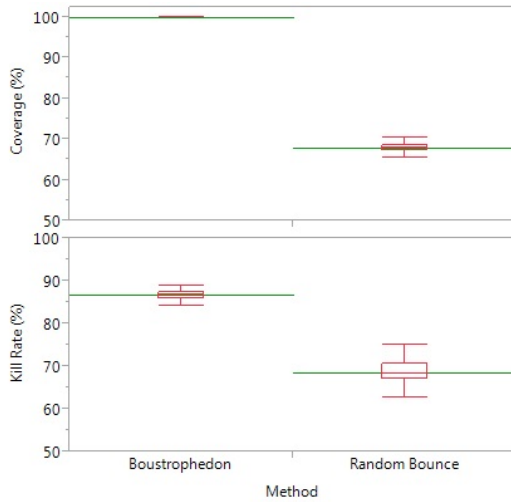


Fig. 11. Comparison of percentage of area covered and percentage of mosquitoes killed for the boustrophedon and random bounce coverage patterns. Plots show aggregate results of 100 trials, using the workspace shown in Fig. 7.

second intervals while the other continuously tracked the voltage across each bug zapper mesh. Both sets of data are time-stamped so that they can be correlated to determine the location of each kill. Fig. 13 shows the ten-minute circuit around a body of water followed in the first trial with the kill locations superimposed upon it.

## VI. CONCLUSION AND FUTURE WORK

Initial tests indicate that we can use our instrumentation to track the location of a mosquito-killing drone as it patrols a field and that we can detect and map mosquito kills. Simulation has shown that covering the field thoroughly leads

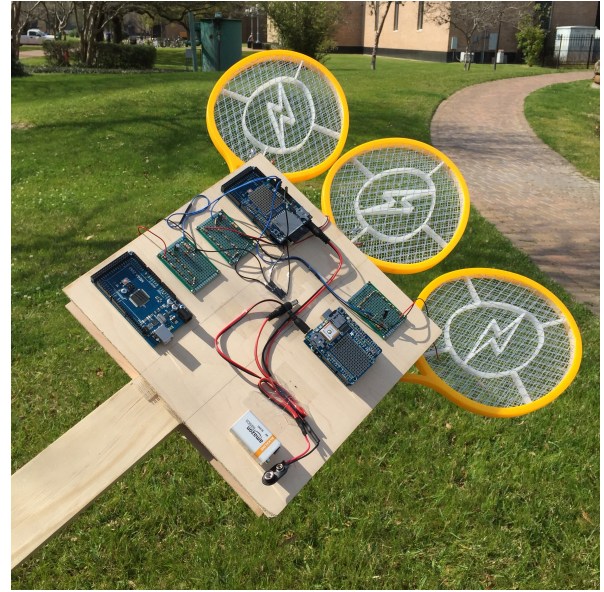


Fig. 12. To calibrate the system, three instrumented bug zappers were carried on a 2.5 m pole.

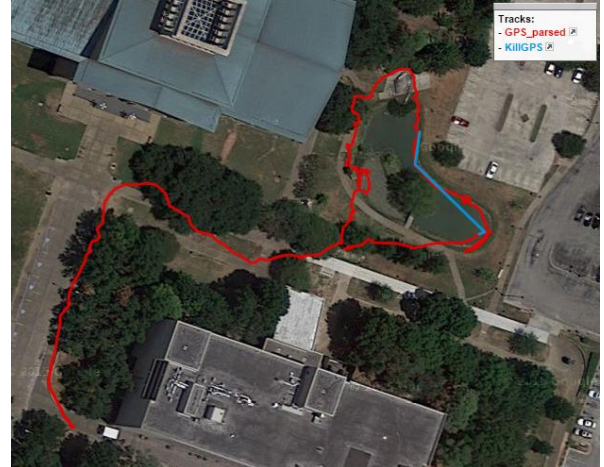


Fig. 13. Map overlaid with GPS path (red line) and kill locations (connected by blue line). Visualization using [18].

to a higher success rate when killing mosquitoes. Because the mosquitoes move around, the robot will not kill all the mosquitoes in a single trial as some can fly into a previously covered area as the robot approaches them; however, the chances of killing the mosquitoes increase as the coverage increases.

There are a number of refinements to the simulation algorithm that could be pursued in future work. The mosquito biasing algorithm could be made less near-sighted and look at an array of pixels further from the current location of the mosquito. Some modifications to the robot flight may force it to take turns more slowly or handle environmental disturbances. A bias away from the robot may be added to the mosquito heading. The model may be expanded to three dimensions. An alternative search path that looks for mosquitoes randomly then exhaustively covers areas dense

in mosquitoes may be compared to the existing algorithms. These and many other considerations may be included to make a more realistic model for future work. Full instrumentation of the multi-copter drone will allow much more extensive testing of the hardware design and will allow field tests of the simulation algorithms.

## REFERENCES

- [1] J. A. Dennett, A. Bala, T. Wuithiranyagool, Y. Randle, C. B. Sargent, H. Guzman, M. SIIRIN, H. K. Hassan, M. Reyna-Navar, T. R. Unnasch *et al.*, "Associations between two mosquito populations and west nile virus in harris county, texas, 2003–06," *Journal of the American Mosquito Control Association*, vol. 23, no. 3, p. 264, 2007.
- [2] R. Peter, P. Van den Bossche, B. L. Penzhorn, and B. Sharp, "Tick, fly, and mosquito control—lessons from the past, solutions for the future," *Veterinary parasitology*, vol. 132, no. 3, pp. 205–215, 2005.
- [3] W. H. Organization, "Guidelines for laboratory and field testing of mosquito larvicides," *WORLD HEALTH ORGANIZATION COMMUNICABLE DISEASE CONTROL, PREVENTION AND ERADICATION WHO PESTICIDE EVALUATION SCHEME*, 2005.
- [4] D. V. Maliti, N. J. Govella, G. F. Killeen, N. Mirzai, P. C. Johnson, K. Kreppel, and H. M. Ferguson, "Development and evaluation of mosquito-electrocuting traps as alternatives to the human landing catch technique for sampling host-seeking malaria vectors," *Malaria journal*, vol. 14, no. 1, p. 1, 2015.
- [5] J. M. Marshall and C. E. Taylor, "Malaria control with transgenic mosquitoes," *PLoS Med*, vol. 6, no. 2, p. e1000020, 2009.
- [6] C. A. Hill, F. C. Kafatos, S. K. Stansfield, and F. H. Collins, "Arthropod-borne diseases: vector control in the genomics era," *Nature Reviews Microbiology*, vol. 3, no. 3, pp. 262–268, 2005.
- [7] P. Anupa Elizabeth, M. Saravana Mohan, P. Philip Samuel, S. Pandian, and B. Tyagi, "Identification and eradication of mosquito breeding sites using wireless networking and electromechanical technologies," in *Recent Trends in Information Technology (ICRTIT), 2014 International Conference on*. IEEE, 2014, pp. 1–6.
- [8] B. Hur and W. Eisenstadt, "Low-power wireless climate monitoring system with rfid security access feature for mosquito and pathogen research," in *Mobile and Secure Services (MOBISERCSERV), 2015 First Conference on*. IEEE, 2015, pp. 1–5.
- [9] C. Boonsri, S. Sumriddetchkajorn, and P. Buranasiri, "Laser-based mosquito repelling module," in *Photonics Global Conference (PGC), 2012*. IEEE, 2012, pp. 1–4.
- [10] J. Kare and J. Buffum, "Build your own photonic fence to zap mosquitoes midflight [backwards star wars]," *IEEE Spectrum*, vol. 5, no. 47, pp. 28–33, 2010. [Online]. Available: <http://spectrum.ieee.org/consumer-electronics/gadgets/backyard-star-wars>
- [11] H. Choset, "Coverage for robotics - a survey of recent results," *Annals of Mathematics and Artificial Intelligence*, vol. 31, no. 1-4, pp. 113–126, October 2001.
- [12] D. Spears, W. Kerr, and W. Spears, "Physics-based robot swarms for coverage problems," *The international journal of intelligent control and systems*, vol. 11, no. 3, 2006.
- [13] S. Koenig, B. Szymanski, and Y. Liu, "Efficient and inefficient ant coverage methods," *Annals of Mathematics and Artificial Intelligence*, vol. 31, no. 1, pp. 41–76, Oct. 2001.
- [14] C. Das, A. Becker, and T. Bretl, "Probably approximately correct coverage for robots with uncertainty," in *IEEE/RSJ International Conference on Intelligent Robots and Systems (IROS)*, vol. 1, San Francisco, CA, USA, Oct. 2011, pp. 1160–1166.
- [15] D.-T. Lee and A. K. Lin, "Computational complexity of art gallery problems," *Information Theory, IEEE Transactions on*, vol. 32, no. 2, pp. 276–282, 1986.
- [16] R. Sollenberger, "Solo specs: Just the facts," May 2015. [Online]. Available: <https://3dr.com/solo-gopro-drone-specs/>
- [17] M. Gillies and T. Wilkes, "The vertical distribution of some West African mosquitoes (Diptera, Culicidae) over open farmland in a freshwater area of The Gambia," *Bulletin of entomological research*, vol. 66, no. 01, pp. 5–15, 1976.
- [18] A. Schneider, "Gps visualizer," Mar. 2003. [Online]. Available: <http://www.gpsvisualizer.com>